Epidemic Processes over Adaptive State-Dependent Networks

Masaki Ogura* and Victor M. Preciado†
University of Pennsylvania. 3330 Walnut Street, Philadelphia, PA 19104. USA.
(Dated: March 1, 2022)

In this paper, we study the dynamics of epidemic processes taking place in adaptive networks of arbitrary topology. We focus our study on the adaptive susceptible-infected-susceptible (ASIS) model, where healthy individuals are allowed to temporarily cut edges connecting them to infected nodes in order to prevent the spread of the infection. In this paper, we derive a closed-form expression for a lower bound on the epidemic threshold of the ASIS model in arbitrary networks with heterogeneous node and edge dynamics. For networks with homogeneous node and edge dynamics, we show that the resulting lower bound is proportional to the epidemic threshold of the standard SIS model over static networks, with a proportionality constant that depends on the adaptation rates. Furthermore, based on our results, we propose an efficient algorithm to optimally tune the adaptation rates in order to eradicate epidemic outbreaks in arbitrary networks. We confirm the tightness of the proposed lower bounds with several numerical simulations and compare our optimal adaptation rates with popular centrality measures.

arXiv:1602.08456v2 [cs.SI] 9 Jun 2016

I. INTRODUCTION

The analysis of dynamic processes taking place in complex networks is a major research area with a wide range of applications in social, biological, and technological systems [1–3]. The spread of information in online social networks, the evolution of an epidemic outbreak in human contact networks, and the dynamics of cascading failures in the electrical grid are relevant examples of these processes. While major advances have been made in this field, most modeling and analysis techniques are specifically tailored to study dynamic processes taking place in static networks. However, empirical observations in social [4–6], biological [7–9], and financial networks [10] illustrate how real-world networks are constantly evolving over time [11]. Unfortunately, the effects of temporal structural variations in the dynamics of networked systems remain poorly understood.

In the context of temporal networks, we are specially interested in the interplay between the dynamics on networks (i.e., the dynamics of processes taking place in the network) and the dynamics of networks (i.e., the temporal evolution of the network structure). Although the dynamics on and of networks are usually studied separately, there are many cases in which the evolution of the network structure is heavily influenced by the dynamics of processes taking place in the network. One of such cases is found in the context of epidemiology, since healthy individuals tend to avoid contact with infected individuals in order to protect themselves against the disease—a phenomenon called *social distancing* [12, 13]. As a consequence of social distancing, the structure of the network adapts to the dynamics of the epidemics taking place in the network. Similar adaptation mechanisms have been studied in the context of power networks [14], biological and neural networks [15, 16] and on-line social networks [17].

Despite the relevance of network adaptation mechanisms, their effects on the network dynamics are not well understood. In this research direction, we find the seminal work by Gross et al. in [18], where a simple adaptive rewiring mechanism was proposed in the context of epidemic models. In this model, a susceptible node can cut edges connecting him to infected neighbors and form new links to *any* randomly selected susceptible nodes—without structural constraint in the formation of new links. Despite its simplicity, this adaptation mechanism induces a complex bifurcation diagram including healthy, oscillatory, bistable, and endemic epidemic states [18]. Several extensions of this work can be found in the literature [19–25], where the authors assume homogeneous infection and recovery rates in the network. Another model that is specially relevant to our work is the adaptive susceptible-infected-susceptible (ASIS) model proposed in [26]. In this model, edges in a given contact network can be temporarily removed in order to prevent the spread of the epidemic. An interesting feature of the ASIS model is that, in contrast with Gross' model, it is able to account for arbitrary contact patterns, since links are constrained to be part of a given contact graph. Despite its modeling flexibility, analytical results for the ASIS model [26, 27] are based on the assumption of homogeneous contact patterns (i.e., the contact graph is complete), as well as homogeneous node and edge dynamics (i.e., nodes present the same infection and recovery rates, and edges share the same adaptation rates).

As a consequence of the lack of tools to analyze network adaptation mechanisms, there is also an absence of effective methodologies for actively utilizing adaptation mechanisms for containing spreading processes. Although we find in the literature a few attempts in this direction, most of them rely on extensive numerical simulations [28], on assuming a homogeneous contact patterns [29], or a homogeneous node and edge dynamics [30]. In contrast, while controlling epidemic processes over static

* ogura@seas.upenn.edu
† preciado@seas.upenn.edu

networks, we find a plethora of tools based on game theory [31, 32] or convex optimization [33, 34].

In this paper, we study adaptation mechanisms over arbitrary contact networks. In particular, we derive an explicit expression for a lower bound on the epidemic threshold of the ASIS model for arbitrary networks, as well as heterogeneous node and edge dynamics. In the case of homogeneous node and edge dynamics, we show that the lower bound is proportional to the epidemic threshold of the standard SIS model over a static network [35]. Furthermore, based on our results, we propose an efficient algorithm for optimally tuning the adaptation rates of an arbitrary network in order to eradicate an epidemic outbreak in the ASIS model. We confirm the tightness of the proposed lower bonds with several numerical simulations and compare our optimal adaptation rates with popular centrality measures.

II. HETEROGENEOUS ASIS MODEL

In this section, we describe the adaptive susceptible-infected-susceptible (ASIS) model over *arbitrary* networks with *heterogeneous* node and edge dynamics (heterogeneous ASIS model for short). We start our exposition by considering a spreading process over a time-varying contact graph $\mathcal{G}(t) = (\mathcal{V}, \mathcal{E}(t))$, where $\mathcal{V} = \{1, \dots, n\}$ is the set of nodes and $\mathcal{E}(t)$ is the time-varying set of edges. For any $t \geq 0$, $A(t) = [a_{ij}(t)]_{i,j}$ corresponds to the adjacency matrix of $\mathcal{G}(t)$, and the neighborhood of node i at time t is defined as $\mathcal{N}_i(t) = \{j : \{i,j\} \in \mathcal{E}(t)\}$. In the standard SIS epidemic model, the state of node i at time t is described by a Bernoulli random variable $x_i(t) \in \{0,1\}$, where node i is said to be *susceptible* if $x_i(t) = 0$, and *infected* if $x_i(t) = 1$. When the contact graph evolves over time, the evolution of x_i is described by a Markov process with the following transition probabilities:

$$\begin{aligned} P(x_i(t+h) = 1 \mid x_i(t) = 0) &= \beta_i \sum_{k \in \mathcal{N}_i(t)} x_k(t)\, h + o(h), \\ P(x_i(t+h) = 0 \mid x_i(t) = 1) &= \delta_i h + o(h), \end{aligned} \tag{1}$$

where the parameters $\beta_i > 0$ and $\delta_i > 0$ are called the *infection* and *recovery* rates of node i.

In the heterogeneous ASIS model, the epidemics takes place over a time-varying network that we model as a continuous-time stochastic graph process $\mathcal{G} = \{\mathcal{G}(t)\}_{t \geq 0}$, described below. Let $\mathcal{G}(0) = (\mathcal{V}, \mathcal{E}(0))$ be an initial connected contact graph with adjacency matrix $A(0) = [a_{ij}(0)]_{i,j}$. We assume that $\mathcal{G}(0)$ is strongly connected. Edges in the initial graph $\mathcal{G}(0)$ appear and disappear over time according to the following Markov processes:

$$\begin{aligned} P(a_{ij}(t+h) = 0 \mid a_{ij}(t) = 1) = \\ \phi_{ij} x_i(t) h + \phi_{ji} x_j(t) h + o(h), \end{aligned} \tag{2}$$

$$P(a_{ij}(t+h) = 1 \mid a_{ij}(t) = 0) = a_{ij}(0) \psi_{ij} h + o(h), \tag{3}$$

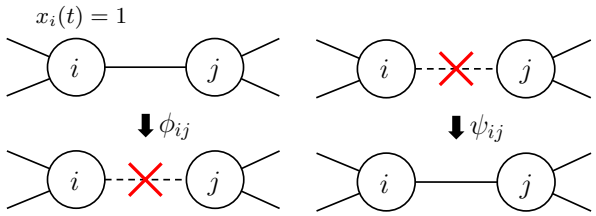


Figure 1: Adaptation mechanisms in the ASIS model.

where the parameters $\phi_{ij} > 0$ and $\psi_{ij} = \psi_{ji} > 0$ are called the *cutting* and *reconnecting* rates. Notice that the transition rate in (2) depends on x_i and x_j, inducing an adaptation mechanism of the network structure to the state of the epidemics. The transition probability in (2) can be interpreted as a protection mechanism in which edge $\{i,j\}$ is stochastically removed from the network if either node i or j is infected. More specifically, because of the first summand (respectively, the second summand) in (2), whenever node i (respectively, node j) is infected, edge $\{i,j\}$ is removed from the network according to a Poisson process with rate ϕ_{ij} (respectively, rate ϕ_{ji}). On the other hand, the transition probability in (3) describes a mechanism for which a 'cut' edge $\{i,j\}$ is 'reconnected' into the network according to a Poisson process with rate ψ_{ij} (see Figure 1). Notice that we include the term $a_{ij}(0)$ in (3) to guarantee that only edges present in the initial contact graph $\mathcal{G}(0)$ can be added later on by the reconnecting process. In other words, we constrain the set of edges in the adaptive network to be a part of the arbitrary contact graph $\mathcal{G}(0)$.

III. EPIDEMIC THRESHOLDS

In this section, we derive a lower bound on the epidemic threshold for the heterogeneous ASIS model. For $\gamma > 0$, let N_γ denote a Poisson counter with rate γ [36]. In what follows, we assume all Poisson counters to be stochastically independent. Then, from the two equations in (1), the evolution of the nodal states can be described by the following set of stochastic differential equations

$$dx_i = -x_i\, dN_{\delta_i} + (1 - x_i) \sum_{k \in \mathcal{N}_i(0)} a_{ik} x_k\, dN_{\beta_i}, \tag{4}$$

for all $i \in \mathcal{V}$. Similarly, from (2) and (3), the evolution of the edges can be described by the following set of stochastic differential equations:

$$da_{ij} = -a_{ij}(x_i\, dN_{\phi_{ij}} + x_j\, dN_{\phi_{ji}}) + (1 - a_{ij})\, dN_{\psi_{ij}}, \tag{5}$$

for all $\{i,j\} \in \mathcal{E}(0)$.

By (4), the expectation $E[x_i]$ obeys the differential equation

$$\frac{d}{dt} E[x_i] = -\delta_i E[x_i] + \beta_i \sum_{k \in \mathcal{N}_i(0)} E[(1 - x_i) a_{ik} x_k].$$

Let $p_i(t) = E[x_i(t)]$ and $q_{ij}(t) = E[a_{ij}(t)x_i(t)]$. Then, it follows that

$$\frac{dp_i}{dt} = -\delta_i p_i + \beta_i \sum_{k\in\mathcal{N}_i(0)} q_{ki} - f_i, \text{ for } i = 1,\dots,n, \quad (6)$$

where

$$f_i(t) = \beta_i \sum_{k\in\mathcal{N}_i(0)} E[x_i(t)x_k(t)a_{ik}(t)]$$

contains positive higher-order terms. In what follows, we derive a set of differential equations to describe the evolution of q_{ij}. From (4) and (5), we obtain the following equation using Itô rule for jump processes (see, e.g., [37])

$$\begin{aligned} d(a_{ij}x_i) =& - a_{ij}x_i\, dN_{\phi_{ij}} - a_{ij}x_i x_j\, dN_{\phi_{ji}} \\ &+ (1-a_{ij})x_i\, dN_{\psi_{ij}} - a_{ij}x_i\, dN_{\delta_i} \\ &+ a_{ij}(1-x_i)\sum_{k\in\mathcal{N}_i(0)} a_{ik}x_k\, dN_{\beta_i}. \end{aligned}$$

Therefore,

$$\begin{aligned} \frac{dq_{ij}}{dt} =& - \phi_{ij}p_{ij} + \psi_{ij}(p_i - q_{ij}) \\ &- \delta_i q_{ij} + \beta_i \sum_{k\in\mathcal{N}_i(0)} q_{ki} - g_{ij}, \end{aligned} \quad (7)$$

for all $\{i,j\} \in \mathcal{E}(0)$, where

$$\begin{aligned} g_{ij}(t) =& \phi_{ji}E[x_i(t)x_j(t)a_{ij}(t)] \\ &+ \beta_i \sum_{k\in\mathcal{N}_i(0)} E\big[x_i(t)x_k(t)a_{ik}(t) \\ &+ (1-a_{ij}(t))a_{ik}(t)x_k(t)\big], \end{aligned}$$

which contains positive higher-order terms. The differential equations (6) and (7) describe the joint evolution of the spreading process and the network structure.

For further analysis, it is convenient to express the differential equations (6) and (7) using vectors and matrices. For this purpose, let us introduce the following notation. Let I_r and $\mathbb{1}_s$ be, respectively, the $r \times r$ identity matrix and the s-dimensional column vector of all ones. Given two matrices M_1 and M_2, their Kronecker product [38] is denoted by $M_1 \otimes M_2$. Given a sequence of matrices $A_1,\dots,A_n$, their direct sum, denoted by $\bigoplus_{i=1}^n A_i$, is defined as the block diagonal matrix having $A_1,\dots,A_n$ as its block diagonals [38]. If $A_1,\dots,A_n$ have the same number of columns, then the matrix obtained by stacking $A_1,\dots,A_n$ in vertical (A_1 on top) is denoted by $\mathrm{col}_{1\le i\le n} A_i = \mathrm{col}(A_1,\dots,A_n)$. Based on this notation, we define the vector-variable $p = \mathrm{col}_{1\le i\le n} p_i$, which contains the infection probabilities of all the nodes in the graph. Similarly, let $q_i = \mathrm{col}_{j\in\mathcal{N}_i(0)} q_{ij}$ and define the column vector $q = \mathrm{col}_{1\le i\le n} q_i$. Define T_i as the unique row-vector satisfying

$$T_i q = \sum_{k\in\mathcal{N}_i(0)} q_{ki}. \quad (8)$$

Note that the length of the row vector T_i and the column vector q equals $2m$, where m is the number of the edges in the initial graph $\mathcal{G}(0)$.

Using this notation, we define the following matrices:

$$B_1 = \begin{bmatrix} \beta_1 T_1 \\ \vdots \\ \beta_n T_n \end{bmatrix}, \quad B_2 = \begin{bmatrix} \beta_1 \mathbb{1}_{d_1} \otimes T_1 \\ \vdots \\ \beta_n \mathbb{1}_{d_n} \otimes T_n \end{bmatrix},$$

$$D_1 = \bigoplus_{i=1}^n \delta_i, \qquad D_2 = \bigoplus_{i=1}^n (\delta_i I_{d_i}),$$

where d_i denotes the degree of node i in the initial graph $\mathcal{G}(0)$. Furthermore, we also define the following matrices

$$\Phi = \bigoplus_{i=1}^n \bigoplus_{j\in\mathcal{N}_i(0)} \phi_{ij},$$

$$\Psi_1 = \bigoplus_{i=1}^n \left(\mathrm{col}_{j\in\mathcal{N}_i(0)} \psi_{ij} \right), \ \Psi_2 = \bigoplus_{i=1}^n \bigoplus_{j\in\mathcal{N}_i(0)} \psi_{ij}.$$

Stacking the set of n differential equations in (6) into a single vector equation, and ignoring the negative higher-order term $-f_i$, we obtain the following entry-wise vector inequality for the probabilities of infection:

$$\frac{dp}{dt} \le -D_1 p + B_1 q. \quad (9)$$

Also, stacking the set of differential equations in (7) with respect to $j \in \mathcal{N}_i(0)$, and ignoring the negative term $-g_{ij}$, we obtain the following entry-wise vector inequality:

$$\frac{dq_i}{dt} \le \mathrm{col}_{j\in\mathcal{N}_i(0)} (\psi_{ij}p_i) - (\phi_{ij}+\delta_i)q_i - \psi_j q_i + \beta_i(\mathbb{1}_{d_i} \otimes T_i)q,$$

where $\psi_i = \bigoplus_{j\in\mathcal{N}_i(0)} \psi_{ij}$. We can further stack the above inequalities with respect to the index i to obtain the following entry-wise vector inequality:

$$\frac{dq}{dt} \le \Psi_1 p + (B_2 - D_2 - \Phi - \Psi_2)q.$$

Combining this inequality and (9), we obtain

$$\frac{d}{dt}\begin{bmatrix} p \\ q \end{bmatrix} \le M \begin{bmatrix} p \\ q \end{bmatrix}, \quad (10)$$

where M is an irreducible matrix (see Appendix A for the proof of irreducibility) defined as

$$M = \begin{bmatrix} -D_1 & B_1 \\ \Psi_1 & B_2 - D_2 - \Phi - \Psi_2 \end{bmatrix}. \quad (11)$$

Therefore, the evolution of the joint vector variable $\mathrm{col}(p,q)$ is upper-bounded by the linear dynamics given by the matrix M. Moreover, the upper bound is tight around the origin, since both f_i and g_{ij} consist of

higher-order terms. From (11), we conclude that the epidemics dies out exponentially fast in the heterogeneous ASIS model if

$$\lambda_{\max}(M) < 0, \tag{12}$$

where $\lambda_{\max}(M)$ is defined as the maximum among the real parts of the eigenvalues of M. Furthermore, since M is a Metzler matrix (i.e., has nonnegative off-diagonals) and irreducible, there is a real eigenvalue of M equal to $\lambda_{\max}(M)$ [38].

In the homogeneous case, where all the nodes share the same infection rate $\beta > 0$ and recovery rate $\delta > 0$, and all the edges share the same cutting rate $\phi > 0$ and reconnecting rate $\psi > 0$, the condition (12) reduces to the following inequality:

$$\frac{\beta}{\delta} < \frac{1+\omega}{\rho}, \tag{13}$$

where ρ is the spectral radius of the initial graph $\mathcal{G}(0)$ and

$$\omega = \frac{\phi}{\delta + \psi},$$

which we call the *effective cutting rate*. The proof of the extinction condition (13) is given in Appendix B. We remark that, in the special case when the network does not adapt to the prevalence of infection, i.e., when $\phi = 0$, we have that $\omega = 0$ and, therefore, the condition in (13) is identical to the extinction condition $\beta/\delta < 1/\rho$ corresponding to the homogeneous networked SIS model over a static network [35].

It is worth comparing the condition in (13) with the epidemic threshold τ_c given in [26] for the case in which $\mathcal{G}(0)$ is the complete graph:

$$\tau_c = \frac{\omega_1 - 1}{n(h(\omega_1; \xi/\delta) - 2 + n^{-1})}, \quad \omega_1 = \frac{2\zeta}{\xi}, \tag{14}$$

where ξ is the link-creating rate, ζ is the link-breaking rate, and h is a positive and "slowly varying" function depending on the metastable long-time average of the number of infected nodes (for details, see [26]). We first notice that our lower bound in (13) can be checked directly from the parameters of the model, namely, the adjacency matrix of the initial graph $\mathcal{G}(0)$ and the relevant rates of the model. This is in contrast with the threshold in (14), since it depends on the metastable average of the number of infected nodes and, thus, can only be computed via numerical simulations. We also remark that the lower bound on the epidemic threshold in (13) and the epidemic threshold in (14) both exhibit affine dependence on the effective link-breaking rates ω and ω_1, respectively. Finally, we see that the recovery rate δ appears in different places in the two conditions, namely, inside the expression of ω in (13) and inside the function h in (14). However, the consequences of this difference are not obvious, since h is defined via the metastable state and, therefore, does not allow an analytical investigation.

We now check the tightness of the lower bound in (13) with numerical simulations. To find the metastable number of infected nodes, we compute the long-time average of the number of infected nodes, defined as

$$y(t) = \frac{1}{t}\int_0^t \sum_{i=1}^{n} x_i(\tau)\, d\tau \tag{15}$$

(for a sufficiently large t). In practice, the epidemics can die out during the simulation due to random fluctuations. To prevent this from happening, we use the procedure in [39], where randomly chosen nodes are immediately reinfected after the infection process dies (i.e., when all the variables $x_1(t), \ldots, x_n(t)$ become zero). To make sure that the process has reached the metastable state, we use the method in [39], where two independent simulations are simultaneously run on the same network. One simulation starts with a 10% of randomly chosen infected nodes, whereas the second simulation starts with all the nodes infected. For each simulation, we compute the long-time average of infected nodes using (15), which we denote by $y_1(t)$ and $y_2(t)$, respectively. Similarly, we compute the long-time average of the number of edges present in the networks using the expression $z(t) = t^{-1}\int_0^t \sum_{i<j} a_{ij}(\tau)\, d\tau$, for each one of the two simulations, which we denote by $z_1(t)$ and $z_2(t)$, respectively. Following the procedure in [39], the simulation is stopped when the following condition is satisfied

$$\frac{|y_1(t) - y_2(t)|}{y_1(t) + y_2(t)} + \frac{|z_1(t) - z_2(t)|}{z_1(t) + z_2(t)} < 10^{-4}.$$

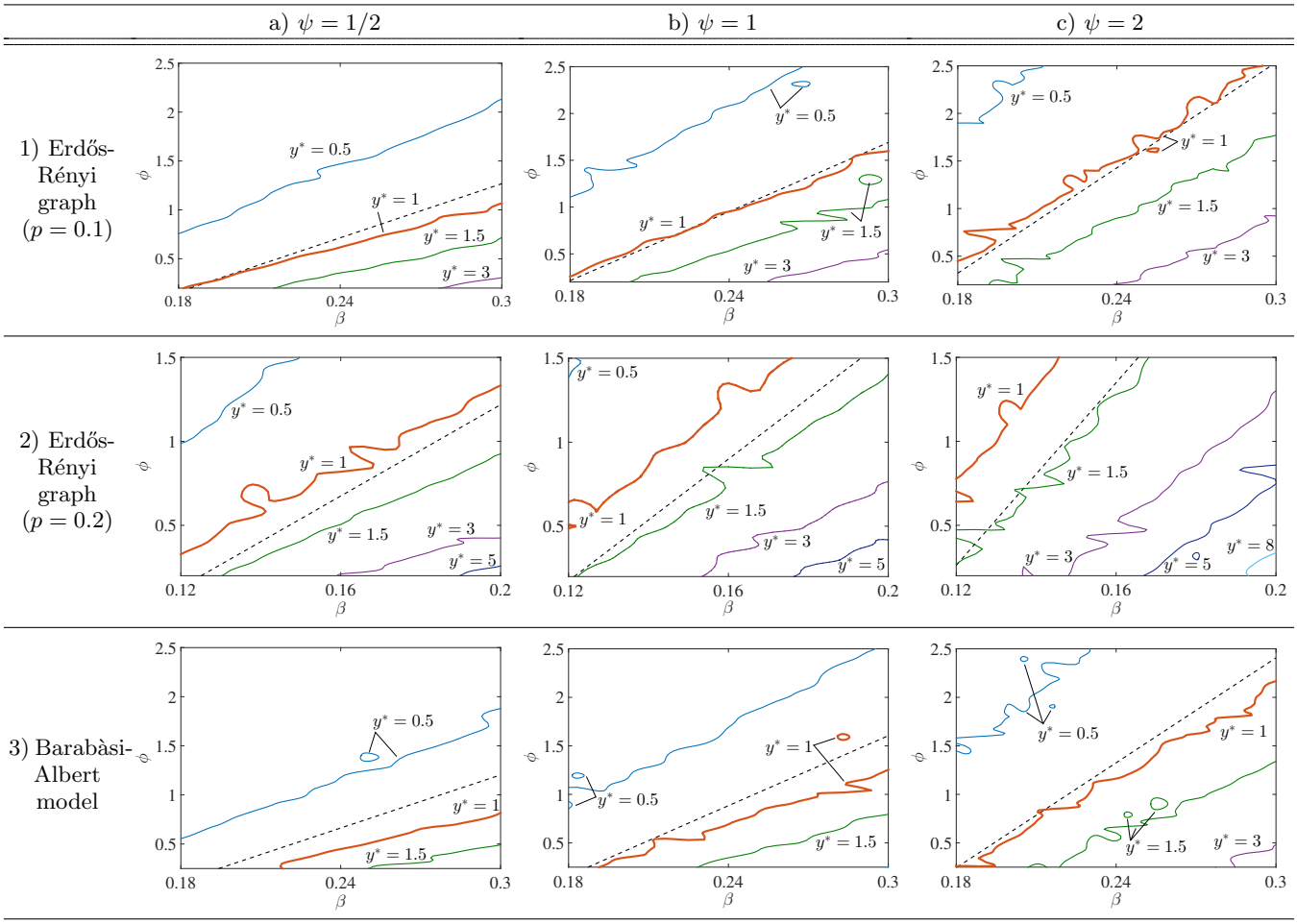
Once the simulation is stopped, the metastable number of infected nodes is determined by

$$y^* = y(t) - 1,$$

where the subtraction of one compensates the effect of the re-infection procedure used in our simulations.

Let the initial graph $\mathcal{G}(0)$ be realizations of the following random graph models with $n = 40$ nodes: *1*) an Erdős-Rényi graph with edge probability $p = 0.1$, *2*) an Erdős-Rényi graph with edge probability $p = 0.2$, and *3*) a Barabàsi-Albert random graph with average degree 3.65. We fix the recovery rate to $\delta = 1$ for all nodes in the graph, for the purpose of illustration. For three different values of the reconnecting rate, $\psi \in \{1/2, 1, 2\}$, we show in Table I the contour plots of the metastable number y^* of infected nodes as we vary the values of the infection rate β and the cutting rate ϕ. We see how the analytical lower bounds (represented as dashed straight lines in the figures in Table I) are in good accordance with the numerical contour corresponding $y^* = 1$ (orange thick curves), in particular for the Erdős-Rényi graph with edge probability $p = 0.1$. For the specific case of $\psi = 1$, Figure 2 shows the values of y^* when $\phi = 1$ (blue line), 2 (orange dashed line), and 3 (green dotted line), and β varies from 0 to 2. The vertical lines in the figure show the theoretical epidemic threshold values of β predicted from the

Table I: y^* versus β and ϕ, with $\delta = 1$. The dashed straight lines show the analytically derived lower bound $(1+\omega)/\rho = \beta$ on the epidemic threshold. The contour plots are obtained by spline-interpolations of the discrete data obtained from the simulations.



lower bound (13). We confirm that these thresholds are in good accordance with the numerical thresholds, which corresponds to the values for which the curves cross the horizontal line $y^* = 1$.

IV. COST-OPTIMAL ADAPTATION FOR EPIDEMIC ERADICATION

Based on our theoretical results in the last section, in this section we study the problem of tuning the rates of the heterogeneous ASIS model in order to eradicate an epidemic outbreak. Specifically, we consider the situation where we can tune the values of the infection, recovery, and cutting rates in the network (for technical reasons, we cannot tune the reconnecting rates in our framework, as we discuss at the end of Appendix C). In this setup, we assume that there is a cost associated with tuning the values of these rates. These costs are described using the following collection of cost functions. The first cost function $f(\beta)$ accounts for the cost of tuning the infection rates in the network to the values in the vector $\beta = (\beta_i)_i$. In other words, if we want to have a network where the infection rates are those in the vector β, we need to pay $f(\beta)$ monetary units. Similarly, the functions $g(\delta)$ and $h(\phi)$ account for the cost of tuning the recovery and the cutting rates to the vectors $\delta = (\delta_i)_i$ and $\phi = (\phi_{ij})_{i,j}$, respectively. Using these cost functions, our objective is to find the cost-optimal investment profile for tuning these rates in order to eradicate the disease at a desired exponential decay rate. From our theoretical analysis, this exponential decay rate is given by $\lambda_{\max}(M)$ in (12). Hence, the optimal tuning problem can be stated as follows:

Problem 1 (Cost-optimal eradication)**.** *Given a desired exponential decay rate $\bar{\lambda} > 0$, and positive numbers $\underline{\beta}$, $\bar{\beta}$, $\underline{\delta}$, $\bar{\delta}$, $\underline{\phi}$, and $\bar{\phi}$, find the set of rates $(\beta_i)_i$, $(\delta_i)_i$, and $(\phi_{ij})_{i,j}$ satisfying the following feasibility bounds*

$$\underline{\beta} \leq \beta_i \leq \bar{\beta},\ \underline{\delta} \leq \delta_i \leq \bar{\delta},\ \underline{\phi} \leq \phi_{ij} \leq \bar{\phi}, \tag{16}$$

such that the infection probabilities p_i in the heterogeneous ASIS model decay to zero exponentially fast at a

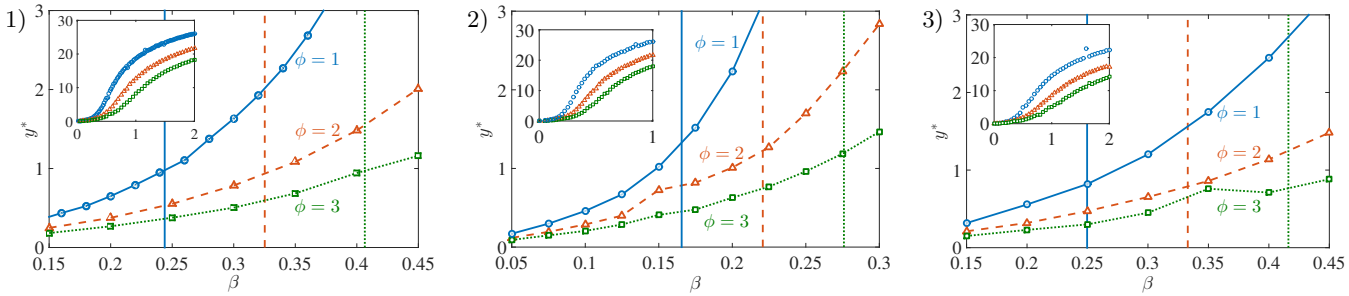


Figure 2: Metastable number of infected nodes versus β for $\phi = 1, 2, 3$ with $\delta = \psi = 1$. 1) Erdős-Rényi graph ($p = 0.1$), 2) Erdős-Rényi graph ($p = 0.2$), and 3) Barabàsi-Albert model.

rate $\bar{\lambda}$, while the total tuning cost

$$C = f(\beta) + g(\delta) + h(\psi)$$

is minimized.

In what follows, we show how this problem can be cast into a type of optimization problems called geometric programs [40], which allows us to find the cost-optimal rates in polynomial time. The techniques herein presented extend those in [34, 41], where the authors proposed the use of convex programming to find the cost-optimal allocation of resources to eradicate an epidemic outbreak in arbitrary *static* networks. The techniques presented below work for a wide family of cost functions, called posynomial functions (see [40] for more details). For simplicity in our exposition, we illustrate the idea behind our approach with these particular cost functions:

$$f(\beta) = c_1 + c_2 \sum_{i=1}^{n} \frac{1}{\beta_i^{p_i}},$$
$$g(\delta) = c_3 + c_4 \sum_{i=1}^{n} \frac{1}{(q_i - \delta_i)^{r_i}},$$
$$h(\phi) = c_5 + c_6 \sum_{\{i,j\} \in \mathcal{G}(0)} \frac{1}{(s_{ij} - \phi_{ij})^{u_{ij}}},$$

where $c_1, \ldots, c_6$ are a set of parameters that are chosen to normalize the cost functions to satisfy the following equalities:

$$f(\bar{\beta}, \ldots, \bar{\beta}) = 0, \quad f(\underline{\beta}, \ldots, \underline{\beta}) = 1,$$
$$g(\bar{\delta}, \ldots, \bar{\delta}) = 1, \quad g(\underline{\delta}, \ldots, \underline{\delta}) = 0,$$
$$h(\bar{\phi}, \ldots, \bar{\phi}) = 1, \quad h(\underline{\phi}, \ldots, \underline{\phi}) = 0,$$

and the constants p_i, q_i, r_i, s_{ij}, and u_{ij} are positive real parameters that can be used to modify the shape of the cost functions. The parameters in f, the function representing the cost of tuning the infection rates, are chosen to make the function decreasing with respect to each β_i. In other words, the higher the tuning investment, the smaller the resulting infection rate (as we should expect in practical situations). Following a similar reasoning, the functions g and ϕ are set to be increasing.

Once the cost functions are selected, we must solve the problem of finding the optimal tuning investment to achieve a desired exponential decay rate in the probabilities of infection. From the inequality in (10), the infection probabilities $p_1, \ldots, p_n$ decay exponentially at a rate (at least) $\bar{\lambda}$ if

$$\lambda_{\max}(M) \leq -\bar{\lambda}. \tag{17}$$

Since M is an irreducible and Metzler matrix, we can use Perron-Frobenius theory [38] to prove that (17) is satisfied if there exists an entry-wise positive vector v satisfying the following entry-wise vector inequality (see [34] for more details):

$$Mv < -\bar{\lambda} v. \tag{18}$$

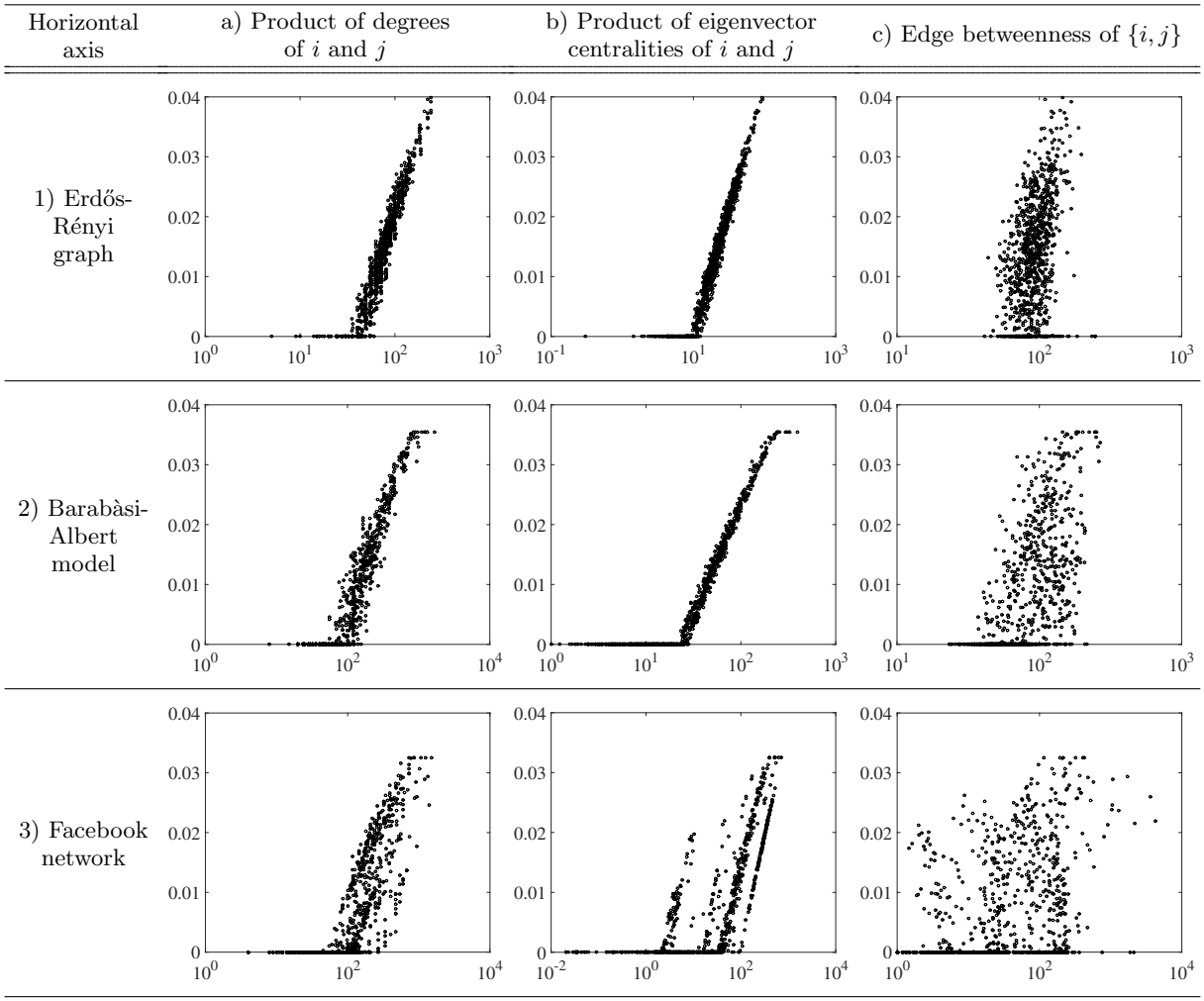
Therefore, Problem 1 can be reduced to the following equivalent optimization problem:

$$\begin{aligned} \underset{\beta,\, \delta,\, \phi,\, v}{\text{minimize}} \quad & f(\beta) + g(\delta) + h(\phi) \\ \text{subject to} \quad & (16),\ (18),\ \text{and } v > 0. \end{aligned} \tag{19}$$

As we show in Appendix C, we can equivalently transform this optimization problem into a geometric program [40], which can be efficiently solved using standard optimization software. The computational complexity of solving the resulting geometric program is $O((n+m)^{7/2})$, where n is the number of nodes and m is the number of edges in the initial network $\mathcal{G}(0)$.

In the rest of this section, we compute the optimal tuning profiles for three different graphs and compare our results with several network centralities. In our simulations, we consider the following three graphs with $n = 247$ nodes: *1)* an Erdős-Rényi graph with 916 edges, *2)* a Barabàsi-Albert random graph with 966 edges, and *3)* a social subgraph (obtained from Facebook) with 947 edges. For simplicity in our simulations, we assume that all nodes share the same recovery rate $\delta = 0.1$ and infection rate $\beta = \delta/(1.1\rho)$, where ρ denotes the spectral radius of each initial graph. Since $\delta/\beta = 1.1\,\rho > \rho$, the extinction condition (13) indicates that the infection process does not necessarily die out without adaptation, i.e., when $\phi_{ij} = 0$. The rest of parameters in our simulations are set as follows: we let $\underline{\phi} = 0$, $\bar{\phi} = 4\beta$, and

Table II: Cost-optimal cutting rates ϕ_{ij}



$\psi_{ij} = \beta$. Also, the parameters in the cost functions are $p_i = q_i = r_i = u_{ij} = 1$ and $s_{ij} = 2\bar{\phi}$. The desired exponential decay rate is chosen to be $\bar{\lambda} = 0.005$.

Using this set of parameters, we solve the optimization problem (19) following the procedure described in Appendix C. Our numerical results are illustrated in various figures included in Table II. Each figure is a scatter plot where each point corresponds to a particular edge $\{i,j\} \in \mathcal{E}(0)$; the ordinate of each point corresponding to its optimal cutting rate ϕ_{ij}, and the abscissa of each point corresponds to a particular edge-centrality measure. In these figures, we use three different edge-centrality measures: a) the product of the degrees of nodes i and j (left column), b) the product of the eigenvector-centralities of nodes i and j (center column), and c) the betweenness centralities of edge $\{i,j\}$ (right column).

In our numerical results, we observe how both degree-based and eigenvector-based edge-centralities are good measures for determining the amount of investment in tuning cutting rates. In contrast, betweenness centrality does not show a significant dependency on the optimal cutting rates. In particular, for the synthetic networks in rows 1) and 2) in Table II, we observe an almost piecewise affine relationship with the centrality measures in columns a) and b). In particular, in these subplots we observe how edges of low centrality require no investment, while for higher-centrality edges, the tuning investment tends to increase affinely as the centrality of the edge increases – as expected. For the real social network in row c), the relationship between investment and centralities is still strong – although not as clear as in synthetic networks. In the scatter plot corresponding to the relationship between the optimal investment and the eigenvector-based centrality in the real social network (lower center figure in Table II), we observe a collection of several stratified parallel lines. We conjecture that each line corresponds to a different community inside the social network; in other words, the relationship between centrality and optimal investment is almost affine inside each community.

V. CONCLUSION

We have studied an *adaptive* susceptible-infected-susceptible (ASIS) model with heterogeneous node and edge dynamics and arbitrary network topologies. We have derived an explicit expression for a lower bound on the epidemic threshold of this model in terms of the maximum real eigenvalue of a matrix that depends explicitly on the network topology and the parameters of the model. For networks with homogeneous node and edge dynamics, the lower bound turns out to be a constant multiple of the epidemic threshold in the standard SIS model over static networks (in particular, the inverse of the spectral radius). Furthermore, based on our results, we have proposed an optimization framework to find the cost-optimal adaptation rates in order to eradicate the epidemics. We have confirmed the accuracy of our theoretical results with several numerical simulations and compare cost-optimal adaptation rates with popular centrality measures in various networks.

[1] D. J. Watts and S. H. Strogatz, Nature **393**, 440 (1998).
[2] M. Newman, A.-L. Barabási, and D. J. Watts, *The Structure and Dynamics of Networks* (Princeton University Press, 2006).
[3] A. Barrat, M. Barthelemy, and A. Vespignani, *Dynamical Processes on Complex Networks* (Cambridge University Press, 2008).
[4] N. Eagle and A. Pentland, Personal and Ubiquitous Computing **10**, 255 (2006).
[5] C. Cattuto, W. van den Broeck, A. Barrat, V. Colizza, J. F. Pinton, and A. Vespignani, PLoS ONE **5** (2010).
[6] N. Santoro, W. Quattrociocchi, P. Flocchini, A. Casteigts, and F. Amblard, in *SNAMAS 2011* (2011) pp. 32–38.
[7] T. M. Przytycka, M. Singh, and D. K. Slonim, Briefings in Bioinformatics **11**, 15 (2010).
[8] J.-D. J. Han, N. Bertin, T. Hao, D. S. Goldberg, G. F. Berriz, L. V. Zhang, D. Dupuy, A. J. M. Walhout, M. E. Cusick, F. P. Roth, and M. Vidal, Nature **430**, 88 (2004).
[9] I. W. Taylor, R. Linding, D. Warde-Farley, Y. Liu, C. Pesquita, D. Faria, S. Bull, T. Pawson, Q. Morris, and J. L. Wrana, Nature Biotechnology **27**, 199 (2009).
[10] L. Sabatelli, S. Keating, J. Dudley, and P. Richmond, The European Physical Journal B **27**, 273 (2002).
[11] P. Holme and J. Saramäki, Physics Reports **519**, 97 (2012).
[12] D. Bell, A. Nicoll, K. Fukuda, P. Horby, A. Monto, F. Hayden, C. Wylks, L. Sanders, and J. Van Tam, Emerging Infectious Diseases **12**, 88 (2006).
[13] S. Funk, M. Salathé, and V. A. A. Jansen, Journal of the Royal Society, Interface / the Royal Society **7**, 1247 (2010).
[14] A. Scirè, I. Tuval, and V. M. Eguíluz, Europhysics Letters **71**, 318 (2005).
[15] J. J. Hopfield, D. I. Feinstein, and R. G. Palmer, Nature **304**, 158 (1983).
[16] W. Schaper and D. Scholz, Arteriosclerosis, Thrombosis, and Vascular Biology **23**, 1143 (2003).
[17] D. Antoniades and C. Dovrolis, Computational Social Networks **2**, 14 (2015).
[18] T. Gross, C. J. D. D'Lima, and B. Blasius, Physical Review Letters **96**, 208701 (2006).
[19] T. Gross and B. Blasius, Journal of the Royal Society, Interface / the Royal Society **5**, 259 (2008).
[20] D. H. Zanette and S. Risau-Gusmán, Journal of Biological Physics **34**, 135 (2008).
[21] V. Marceau, P. A. Noël, L. Hébert-Dufresne, A. Allard, and L. J. Dubé, Physical Review E **82**, 036116 (2010).
[22] C. Lagorio, M. Dickison, F. Vazquez, L. A. Braunstein, P. A. Macri, M. V. Migueles, S. Havlin, and H. E. Stanley, Physical Review E **83**, 026102 (2011).
[23] T. Rogers, W. Clifford-Brown, C. Mills, and T. Galla, Journal of Statistical Mechanics: Theory and Experiment **2012**, P08018 (2012).
[24] D. Juher, J. Ripoll, and J. Saldaña, Journal of Mathematical Biology **67**, 411 (2013).
[25] I. Tunc and L. B. Shaw, Physical Review E **90**, 022801 (2014).
[26] D. Guo, S. Trajanovski, R. van de Bovenkamp, H. Wang, and P. Van Mieghem, Physical Review E **88**, 042802 (2013).
[27] S. Trajanovski, D. Guo, and P. Van Mieghem, Physical Review E **92**, 030801 (2015).
[28] Y. Bu, S. Gregory, and H. L. Mills, Physical Review E **88**, 042801 (2013).
[29] S. Maharaj and A. Kleczkowski, BMC Public Health **12**, 679 (2012).
[30] L. D. Valdez, P. A. Macri, and L. A. Braunstein, Physical Review E **85**, 036108 (2012).
[31] S. Trajanovski, Y. Hayel, E. Altman, H. Wang, and P. Van Mieghem, IEEE Transactions on Control of Network Systems **2**, 406 (2015).
[32] J. Aspnes, K. Chang, and A. Yampolskiy, Journal of Computer and System Sciences **72**, 1077 (2006).
[33] C. Nowzari, V. M. Preciado, and G. J. Pappas, IEEE Control Systems **36**, 26 (2016).
[34] V. M. Preciado, M. Zargham, C. Enyioha, A. Jadbabaie, and G. J. Pappas, IEEE Transactions on Control of Network Systems **1**, 99 (2014).
[35] P. Van Mieghem, J. Omic, and R. Kooij, IEEE/ACM Transactions on Networking **17**, 1 (2009).
[36] W. Feller, *An Introduction to Probability Theory and Its Applications* (John Wiley & Sons, 1956).
[37] F. B. Hanson, *Applied Stochastic Processes and Control for Jump-Diffusions: Modeling, Analysis and Computation* (Society for Industrial and Applied Mathematics, 2007).
[38] R. Horn and C. Johnson, *Matrix Analysis* (Cambridge University Press, 1990).
[39] E. Cator, R. van de Bovenkamp, and P. Van Mieghem, Physical Review E **87**, 062816 (2013).
[40] S. Boyd, S.-J. Kim, L. Vandenberghe, and A. Hassibi, Optimization and Engineering **8**, 67 (2007).
[41] V. M. Preciado, M. Zargham, C. Enyioha, A. Jadbabaie, and G. J. Pappas, in *52nd IEEE Conference on Decision and Control* (2013) pp. 7486–7491.

[42] L. Farina and S. Rinaldi, *Positive Linear Systems: Theory and Applications* (Wiley-Interscience, 2000).
[43] M. Ogura and V. M. Preciado, to appear in IEEE Transactions on Control of Network Systems (2016).

Appendix A: Irreducibility of M

We show that the matrix M defined in (11) is irreducible, that is, there is no similarity transformation that transforms M into a block upper-triangular matrix. For this purpose, define

$$L = \begin{bmatrix} O & T \\ J & S \end{bmatrix},$$

where $J = \bigoplus_{i=1}^{n} \mathbb{1}_{d_i}$, $T = \mathrm{col}_{1\le i\le n} T_i$, and $S = \mathrm{col}_{1\le i\le n}(\mathbb{1}_{d_i} \otimes T_i)$. Since the rates β_i and ψ_{ij} are positive, if $M_{ij} = 0$, then $L_{ij} = 0$ for all distinct i and j. Therefore, to prove the irreducibility of M, it is sufficient to show that L is irreducible.

In order to show that L is irreducible, we shall show that the directed graph $\mathcal{H}$ on the nodes $1, \dots, n+2m$, defined as the graph having adjacency matrix $L \in \mathbb{R}^{(n+2m)\times(n+2m)}$, is strongly connected. We identify the nodes $1, \dots, n+2m$ and variables $p_1, \dots, p_n$, q_{1j} $(j \in \mathcal{N}_1(0))$, $\dots$, q_{nj} $(j \in \mathcal{N}_n(0))$. Then, the upper-right block T of the matrix L indicates that the graph $\mathcal{H}$ contains the directed edge (p_i, q_{ji}) for all $i = 1, \dots, n$ and $j \in \mathcal{N}_i(0)$. Similarly, from the matrices J and S in M, we see that $\mathcal{H}$ contains the directed edges (q_{ij}, p_i) and (q_{ij}, q_{ki}) for all $i = 1, \dots, n$ and $j, k \in \mathcal{N}_i(0)$.

Using these observations, let us first show that $\mathcal{H}$ has a directed path from p_i to p_j for all $i, j \in \{1, \dots, n\}$. Since $\mathcal{G}(0)$ is strongly connected, it has a path $(i_0, \dots, i_\ell)$ such that $i_0 = i$ and $i_\ell = j$. Therefore, from the above observations, we see that $\mathcal{H}$ contains the directed path $(p_i, q_{i_1,i_0}, q_{i_2,i_1}, \dots, q_{i_\ell,i_{\ell-1}}, p_j)$. In the same way, we can show that $\mathcal{H}$ also contains the directed path $(p_i, q_{ji}, q_{ij}, p_i)$ for every $\{i, j\} \in \mathcal{E}(0)$. These two types of directed paths in $\mathcal{H}$ guarantees that $\mathcal{H}$ is strongly connected. Hence the matrix L is irreducible, as desired.

Appendix B: Derivation of (13)

In the homogeneous case, the matrix M takes the form

$$M = \begin{bmatrix} -\delta I & \beta T \\ \psi J & \beta S - (\delta + \phi + \psi) I \end{bmatrix}.$$

In what follows, we show that $\lambda_{\max}(M) < 0$ if and only if (13) holds true.

Since $\mathcal{G}(0)$ is strongly connected by assumption, its adjacency matrix $A(0)$ is irreducible and therefore has an entry-wise positive eigenvector v corresponding to the eigenvalue ρ (see [42]). Define the positive vector $w = \mathrm{col}_{1\le i\le n}(v_i \mathbb{1}_{d_i})$. Then, the definition of T_i in (8) shows $T_i w = \sum_{k\in\mathcal{N}_i(0)} w_{ki} = \sum_{k\in\mathcal{N}_i(0)} v_k = (Av)_i = \rho v_i$ and therefore $Tw = \lambda v$. In the same manner, we can show that $Sw = \rho w$. Moreover, it is straightforward to check that $Jv = w$. Therefore, for a real number c, it follows that

$$M \begin{bmatrix} cv \\ w \end{bmatrix} = \begin{bmatrix} (\beta\rho - c\delta)v \\ (c\psi + \beta\rho - (\delta + \phi + \psi))\, w \end{bmatrix}.$$

Hence, if a real number λ satisfies the following equations:

$$\beta\rho - c\delta = c\lambda,\ c\psi + \beta\rho - (\delta + \phi + \psi) = \lambda, \qquad \text{(B1)}$$

then $\mathrm{col}(cv, w)$ is an eigenvector of M. Since M is irreducible (shown in Appendix A), by Perron-Frobenius theory [38], if $c > 0$ then $\lambda_{\max}(M) = \lambda$ (see [42, Theorem 17]). This, in particular, shows that $\lambda_{\max}(M) < 0$ if and only if there exist $c > 0$ and $\lambda < 0$ such that (B1) holds.

The two equations in (B1) have two pairs of solutions (c_1, λ_1) and (c_2, λ_2) such that $c_1 < 0, \lambda_1 < 0$, and $c_2 > 0$. Therefore, we need to show $\lambda_2 < 0$ if and only if (13) holds true. To see this, we notice that λ_1 and λ_2 are the solutions of the quadratic equation $\lambda^2 + (2\delta + \phi + \psi - \beta\rho)\lambda + \delta(\delta + \phi + \psi) - \beta\rho(\delta + \psi) = 0$ following from (B1). Since $\lambda_1 < 0$, we have $\lambda_2 < 0$ if and only if the constant term $\delta(\delta + \phi + \psi) - \beta\rho(\delta + \psi)$ of the quadratic equation is positive, which is indeed equivalent to (13). This completes the proof of the extinction condition stated in (13).

Appendix C: Geometric Programming

We first give a brief review of geometric programs [40]. Let $x_1, \dots, x_n$ denote positive variables and define $x = (x_1, \dots, x_n)$. We say that a real function $g(x)$ is a *monomial* if there exist $c \ge 0$ and $a_1, \dots, a_n \in \mathbb{R}$ such that $g(x) = c x_1^{a_1} \cdots x_n^{a_n}$. Also, we say that a function $f(x)$ is a *posynomial* if it is a sum of monomials of x (we point the readers to [40] for more details). Given a collection of posynomials $f_0(x)$, $\dots$, $f_p(x)$ and monomials $g_1(x)$, $\dots$, $g_q(x)$, the optimization problem

$$\begin{aligned} \underset{x}{\text{minimize}}\ & f_0(x) \\ \text{subject to}\ & f_i(x) \le 1, \quad i = 1, \dots, p, \\ & g_j(x) = 1, \quad j = 1, \dots, q, \end{aligned}$$

is called a *geometric program*. A constraint of the form $f(x) \le 1$ with $f(x)$ being a posynomial is called a posynomial constraint. Although geometric programs are not convex, they can be efficiently converted into equivalent convex optimization problems [40].

In the following, we rewrite the optimization problem (19) into a geometric program using the new variables $\tilde{\delta}_i = q_i - \delta_i$ and $\tilde{\phi}_{ij} = s_{ij} - \phi_{ij}$. By (16), these

variables should satisfy the constraints

$$q_i - \bar{\delta} \leq \tilde{\delta}_i \leq q_i - \underline{\delta}, \tag{C1}$$
$$s_{ij} - \bar{\phi} \leq \tilde{\phi}_{ij} \leq s_{ij} - \underline{\phi}. \tag{C2}$$

Also, using these variables, the cost function C can be written as $C(\beta, \tilde{\delta}, \tilde{\psi}) = f(\beta) + \tilde{g}(\tilde{\delta}) + \tilde{h}(\tilde{\psi})$, where

$$\tilde{g}(\tilde{\delta}) = c_3 + c_4 \sum_{i=1}^{n} \frac{1}{\tilde{\delta}_i^{r_i}}, \quad \tilde{h}(\tilde{\phi}) = c_5 + c_6 \sum_{\{i,j\} \in \mathcal{G}(0)} \frac{1}{\tilde{\phi}_{ij}^{u_{ij}}}$$

are posynomials. In order to rewrite the constraint (18), we first define the matrices

$$\tilde{D}_1 = \bigoplus_{i=1}^{n} \tilde{\delta}_i, \quad \tilde{D}_2 = \bigoplus_{i=1}^{n} (\tilde{\delta}_i I_{d_i}),$$
$$\tilde{\Phi} = \bigoplus_{i=1}^{n} \bigoplus_{j \in \mathcal{N}_i} \tilde{\phi}_{ij}, \quad \tilde{\Psi}_2 = \bigoplus_{i=1}^{n} \bigoplus_{j \in \mathcal{N}_i(0)} \tilde{\psi}_{ij}.$$

We also introduce the positive constants $\bar{q} = \max_i q_i$, $\bar{\psi} = \max_{i,j} \psi_{ij}$, $\bar{s} = \max_{ij} \bar{s}_{ij}$. Now, adding $(\bar{q} + \bar{\psi} + \bar{s})v$ to both sides of (18), we equivalently obtain

$$\tilde{M} v < (\bar{q} + \bar{\psi} + \bar{s}) v, \tag{C3}$$

where $\tilde{M} = M + (\bar{q} + \bar{\psi} + \bar{s})I$ is given by

$$\tilde{M} = \begin{bmatrix} \tilde{D}_1 + (\bar{q}I - Q_1) + (\bar{\psi} + \bar{s})I & B_1 \\ \Psi_1 & B_2 + \tilde{D}_2 + (\bar{q}I - Q_2) + \tilde{\Phi} + (\bar{s}I - S) + (\bar{\psi}I - \Psi_2) + \lambda I \end{bmatrix}.$$

Summarizing, we have shown that the optimization problem (19) is equivalent to the following optimization problem with (entry-wise) positive variables:

$$\begin{aligned} \underset{\beta, \tilde{\delta}_i, \tilde{\phi}_{ij}, v}{\text{minimize}} \quad & f(\beta) + \tilde{g}(\tilde{\delta}) + \tilde{h}(\tilde{\psi}) \\ \text{subject to} \quad & (16), \text{(C1)}, \text{(C2)}, \text{and (C3)}. \end{aligned} \tag{C4}$$

In this optimization problem, the objective function is a posynomial in the variables β, $\tilde{\delta}$, and $\tilde{\phi}$. Also, the box constraints (16), (C1), and (C2) can be written as posynomial constraints [40]. Finally, since each entry of the matrix $\tilde{M}$ is a posynomial in the variables β, $\tilde{\delta}$, and $\tilde{\phi}$, the vector-constraint (C3) yields $n + 2m$ posynomial constraints. Therefore, the optimization problem (C4) is a geometric program, as desired. Furthermore, a standard estimate on the computational complexity of solving geometric program (see, e.g., [43, Proposition 3]) shows that the computational complexity of solving the optimization problem in (C4) is given by $O((n+m)^{7/2})$.

Finally we remark that $\tilde{M}$ contains both the terms ψ_{ij} and $-\psi_{ij}$ so that we cannot use ψ_{ij} as the decision variable in the geometric program (C4) due to the positivity constraint on decision variables. By this reason, we cannot design the reconnecting rates ψ_{ij} under the framework presented in this paper. This issue is left as an open problem.